Liquid-Phase Dispersion in Packed Beds with Two-Phase Flow

I. A. FURZER and R. W. MICHELL

University of Sydney, Sydney, Australia

Liquid-phase Peclet numbers have been measured for ¼ in. Raschig rings with countercurrent air flow in a 2 in. I.D. column. The response curve has been analyzed by a computer program, since the output data was collected directly on paper tape. The Peclet number calculated from a moments analysis is considered unreliable, and the diffusion model can be rejected for the liquid phase. If the Peclet number is calculated by a least-squares fit, and if the result is forced through the peak in the response curve, then a correlation for over one hundred runs with gas flows from 0 to 99% of flooding is given by Equations (7) and (8).

The packed column with two-phase flow is widely used as an item of mass transfer equipment, but the flow pattern in both phases is poorly understood. The liquid phase often flows by gravity through the bed and is described as trickle flow. The liquid path is probably a large number of laminar films which, after a passage through the bed, are partly transferred to the wall. When the ratio of column diameter to nominal packing size exceeds 8 to 1, there is only a small fraction of liquid on the wall after several column diameters, even for a single point liquid distributor. A study of the residence time distribution in the liquid phase shows a considerable departure from plug flow, and the dispersion is often characterized by a dispersion coefficient. Studies of this dispersion should lead to an improved understanding of the mass transfer operation.

There has been reported in the literature a large number of experiments on dispersion in packed beds with single-phase flow. The published results on two-phase flow include the gas-phase dispersion measurements of DeMaria and White (*15*) and Sater and Levenspiel (*11*). The liquid-phase dispersion measurements with two-phase flow includes several individual measurements by Danckwerts (*2*) and Kramers and Alberda (*8*), and the more extensive results of Otake and Kunugita (*9, 10*), Dunn et al. (*3*), Hoogendoorn and Lips (*7*), Sater and Levenspiel (*11*), and de Waal and van Mameran (*13*).

A large number of models have been examined to characterize the dispersion by comparing the input, output responses of the bed. With single-phase flow, a diffusion model has been satisfactory in modeling the output response for pulse, step, and sinusoidal input signals, although Carberry and Bretton (*1*) have noted some anomalous behavior. The situation is not so clear with two-phase flow. Hoogendoorn and Lips (*7*) and Otake and Kunugita (*9*) have found that the diffusion model is unsatisfactory owing to the output response having a long tail for a pulse input signal. Dunn et al. (*3*) have used a step change for an input, and they found the diffusion model did not fit the output response exactly, although it was the best model examined. Sater and Levenspiel (*11*) reported long tails on two output responses at different positions along the bed for a near pulse input signal.

The output signals mentioned have been recorded on a strip chart, and the lines fluctuate about a mean position both for a radioactive sensor used by Sater and Levenspiel (*11*) and a conductivity cell by Dunn et al. (*3*). An explanation of the fluctuation could be owing to the sensitivity of the experimental techniques or the discrete movements in the liquid flow pattern, again reflecting some doubt on the diffusion model.

Dunn et al. (*3*) have calculated the Peclet numbers from the midpoint slope of the output curves and plotted Peclet number against liquid flow rate. There is a large amount of scatter in the result. Sater and Levenspiel (*11*) have correlated the Peclet number with the liquid Reynolds number, the Galileo number, and the group $(a_c d)$. Once again there is considerable scatter, and the exponents on the dimensionless numbers have wide confidence limits. Furzer and Ho (*5*) have found that the liquid-phase Peclet number obtained from Sater and Levenspiel's correlation is too low to explain their distillation results. There appears to be sufficient uncertainty about the diffusion model and the existing correlations to warrant further investigation.

EXPERIMENTAL APPARATUS

A 2 in. I.D. glass column was packed to a depth of 5 ft. with ¼ in. ceramic Raschig rings, as shown in Figure 1. Water was pumped from a reservoir through a rotameter to a liquid distributor. Air was passed through a rotameter and entered below the packing. Both rotameters were calibrated in position. A pressurized reservoir of salt (sodium chloride) solution was connected to a solenoid valve which was attached to the liquid supply line close to the distributor. A process timer was used to energize the valve for 0.3 sec. The packing support contained a covered gas riser and four liquid downcomers. The downcomers fed a small vessel fitted with two electrodes. One electrode consisted of a platinum wire sealed in glass with the exposed wire end coated with platinum black. The other electrode was a 1 in. length of platinum wire coated with platinum black. The electrodes were connected to a Philips conductivity bridge and the D.C. output was passed through a high stability resistor. The voltage drop over the resistor was scanned at the rate of 1/sec. and measured on a digital voltmeter (D.V.M.) which was connected to a paper tape punch.

EXPERIMENTAL PROCEDURE

The response of the electrodes was measured by increasing the scanning rate to 25/sec. and producing a step change in conductivity by rapidly passing the point electrode through a liquid surface. The rise time was less than 40 msec., the minimum time for one scan. The electrodes were placed in the vessel under the packing support and calibrated by circulating salt solutions of known composition. The calibration curve was linear.

The preliminary runs on the column were made by synchronizing the opening of the solenoid valve and the start of the scanner. The admitted pulse of tracer then passed through the column, and the output response was detected by the electrodes. A disturbance in the liquid film on the wall of the column appeared after the pulse of tracer was admitted. This was probably due to a small change in the liquid flow rate due to the entry of the pulse of tracer. The velocity of the disturbance was found to agree with the

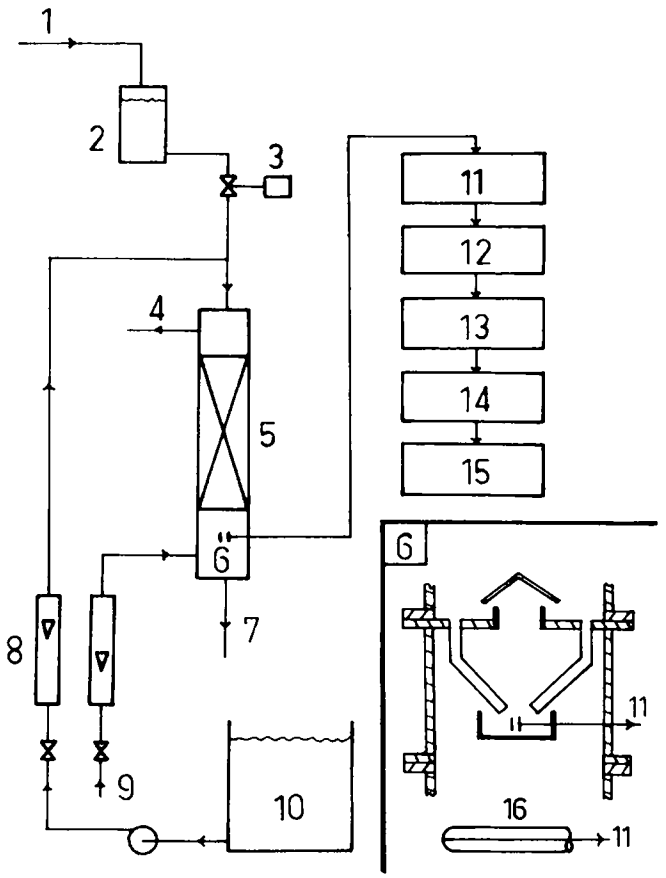

Fig. 1. Schematic diagram of experimental apparatus. 1—air pressure supply, 2—tracer reservoir, 3—solenoid valve, 4—air exit 5—packed column 6—electrodes, 7—water exit, 8—rotameters, 9—air inlet, 10—water reservoir, 11—conductivity bridge, 12—scanner, 13—digital voltmeter, 14—paper tape punch, 15—paper tape output, 16—point electrode.

minimum response time of the system, so the wall flow had the highest velocity of all the fluid elements passing through the column. The column was then filled with water, and the water flow was started during draining and the observations repeated. In this case no liquid disturbance was visible, and there was a large increase in the minimum residence time. The output results were highly reproducible. It would appear that a prerequisite for consistent response curves is that the packing should be wet by flooding or by filling the column with liquid. Under these conditions, the liquid distribution in the column has

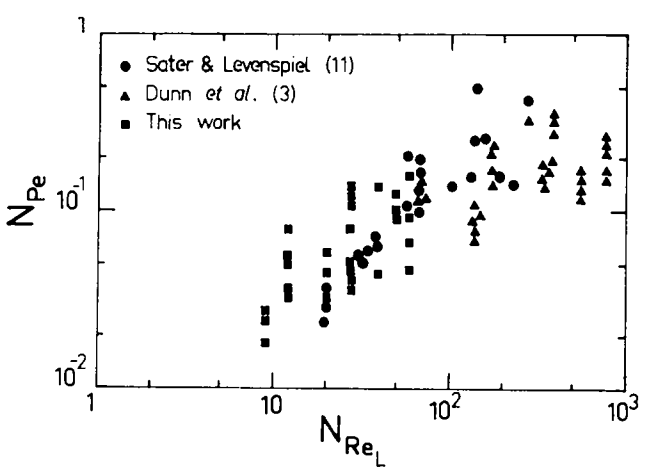

Fig. 2. Peclet number by second moment vs. Reynolds number.

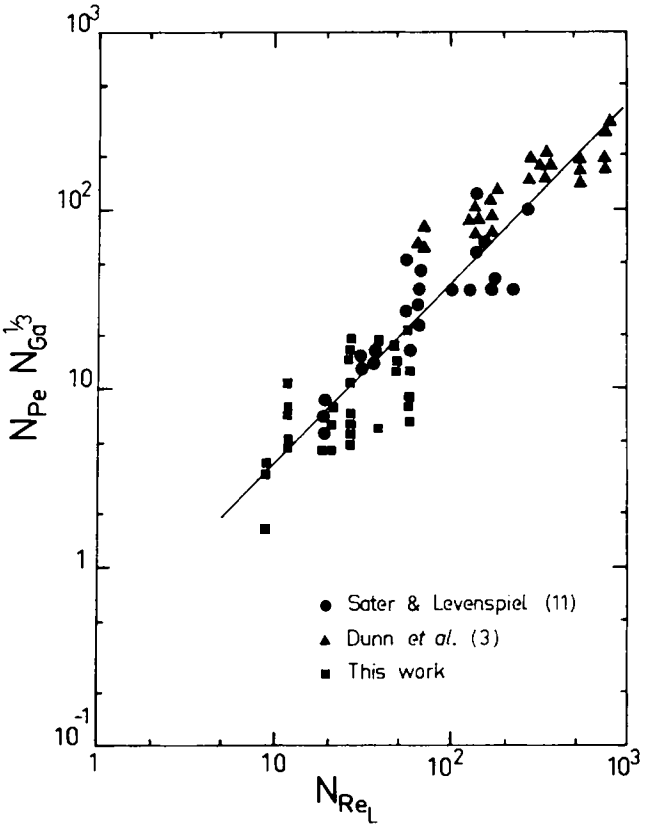

Fig. 3. $N_{Pe}\ N_{Ga}^{1/3}$ (N_{Pe} by second moment) vs. Reynolds number.

reached a stable condition.

A wide range of liquid and gas flow rates were covered from 0 to 99% of the flooding velocities. Thirty-two points were covered and generally triplicate measurements were taken, so over a hundred runs were completed. Seven liquid flow rates varying from 1,000 to 6,680 lb./hr. sq. ft. were used with gas flow rates from 0 to 563 lb./hr. sq. ft. To study the effect of the gas rate on the liquid-phase dispersion, particular attention was given to the flooding conditions. The column was operated with a gas flow just below the flooding point over a wide range of liquid loadings when the pressure drop was in excess of 2 in. water gauge/foot of packing.

A mass balance for the tracer over an element of the bed leads to the following linear partial differential equation:

$$\frac{\partial c}{\partial t} = D\frac{\partial^2 c}{\partial x^2} - u\frac{\partial c}{\partial x} \qquad (1)$$

A test on the linearity of this system was made by admitting pulses of tracer of known size and by recording the maximum concentration of the response curve. This was done by operating the D.V.M. in the maximum mode, whereby the maximum voltage was retained. A plot of pulse size against maximum voltage was linear over a wide range of pulse sizes. It was also found that any point on the output response was proportional to the size of the admitted pulse; this confirms the linearity of the system.

RESULTS

The Peclet number was calculated by the relationship between the second movement of the response curve and the Peclet number as given by van der Laan (*14*):

$$\sigma^2 = \frac{2}{N^2_{Pe}}\left[N_{Pe} - 1 + e^{-N_{Pe}}\right] \qquad (2)$$

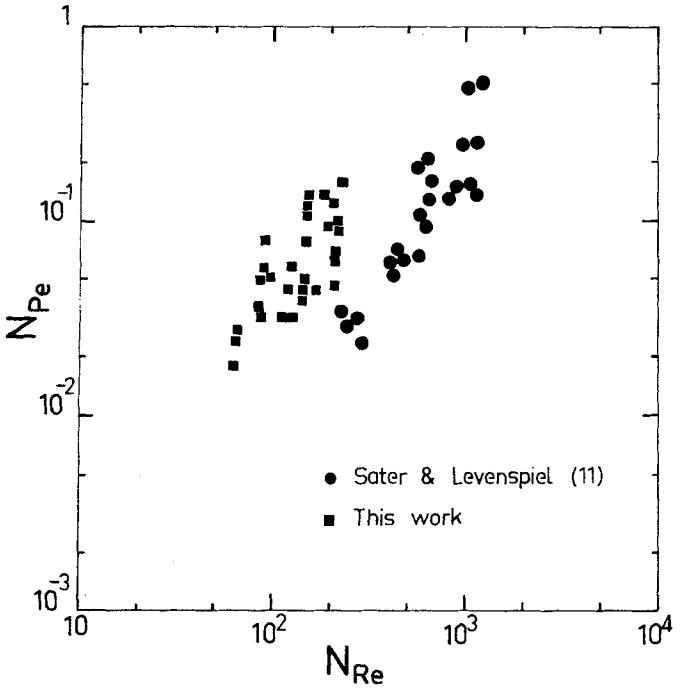

Fig. 4. Peclet number by second moment vs. Reynolds number based on interstitial velocity.

To evaluate the second moment, either the curve is truncated when it returns to its original value, or an exponential curve can be fitted by following Sater and Levenspiel (*11*). Since the response curve had been collected on paper tape, it was convenient to use a statistical method for truncation. A sample of ten points from the response curve was compared with the same size sample at the start of the run. The means and variance of the two samples were compared on an F and t test. If there were a statistically significant difference, then the time was increased by 1 sec. and the process repeated. By this method the moving means and moving variances were examined until there were no significant differences. The Peclet number was then calculated and plotted against the Reynolds number in Figure 2. There is considerable scatter in the results. Also in the same figure are the results of Sater and Levenspiel (*11*) for ½ in. Raschig rings and Dunn et al. (*3*) for 1 and 2 in. Raschig rings. The scatter of these results is comparable with our results on ¼ in. Raschig rings.

A dimensional analysis including the gravitational acceleration results in $N_{Pe} = f(N_{Re}, N_{Ga})$ where N_{Ga} is the Galileo number, a combination of the Froude and Reynolds numbers. Otake and Kunugita (9) found the same form of correlation, with a minus one-third exponent on the Galileo number. A plot of $N_{Pe}\ N_{Ga}^{1/3}$ against the Reynolds number based on the liquid loading is given in Figure 3, and a line of unit slope gives a correlation:

$$N_{Pe} = 3.8\ N_{ReL}\ N_{Ga}^{-1/3} \qquad (3)$$

Once again, there is considerable scatter in the results.

The mean residence time can be evaluated from the first moment of the response curve, and the mean or interstitial liquid velocity is given by

$$u = \frac{Z}{t_M} \qquad (4)$$

A plot of the Peclet number against the Reynolds number based on the interstitial velocity is shown in Figure 4. The scatter is comparable with the data of Sater and Levenspiel (*11*). A plot of $N_{Pe}\ N_{Ga}^{1/3}$ against the same Reynolds number in Figure 5 can be correlated by

$$N_{Pe} = 0.058\ N_{Re}\ N_{Ga}^{-1/3} \qquad (5)$$

This result is considerably different from the correlation by Otake and Kunugita of

$$N_{Pe} = 1.90\ N_{Re}^{1/2}\ N_{Ga}^{-1/3} \qquad (6)$$

However, there is considerable doubt about the exponent of the Reynolds number due to the scatter.

FURTHER ANALYSIS OF THE SYSTEM RESPONSE

The mean residence time calculated from the first moment is reproducible and has a small standard deviation. The results for triplicate runs at a liquid flow rate of 2,330 lb./hr.sq.ft., and with no air are 84.9, 84.4, and 81.6 sec. A plot of the mean residence times against liquid flow rate is a smooth curve with a minimum of scatter. This would indicate that the scatter in the previous figures was due to different values of the second moment which are used to calculate the Peclet number. The major source of this difference is the different truncation times. If the significance levels are altered in the statistical test used for the truncation, then there is a large change in the second moment due to this tailing effect.

Substitution of the Peclet number which had been obtained by the truncation method into a solution of the partial differential equation gives a theoretical response which is considerably different from the measured response. In all runs the spread of the residence times for the theoretical response was larger than the spread of the measured response, or the Peclet number calculated from the second moment is smaller than the real value.

Three methods were used to evaluate the best Peclet number:

1. Minimize the sum of the squares of the differences of the logarithm of the theoretical and measured concentration by using the truncation test.
2. As above but force the result through the maximum point in the response curve.
3. Minimize the sum of the squares of the differences of the concentrations by using the truncation test and by

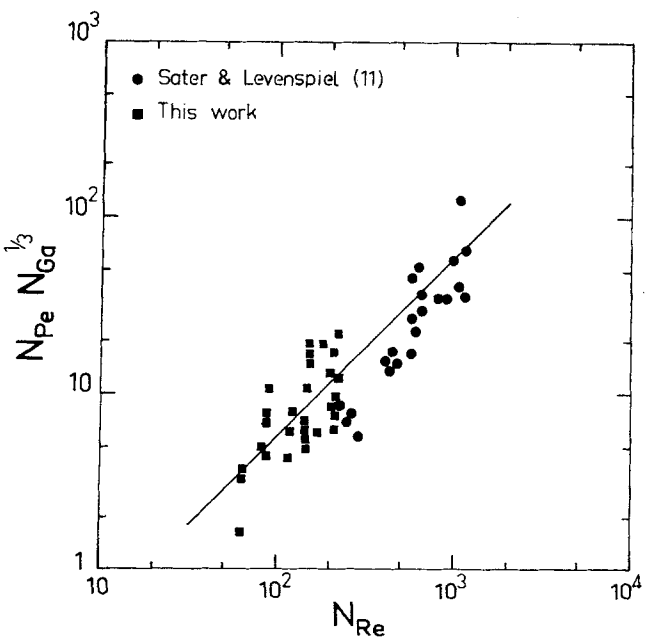

Fig. 5. $N_{Pe}\ N_{Ga}^{1/3}$ (N_{Pe} by second moment) vs. Reynolds number based on interstitial velocity.

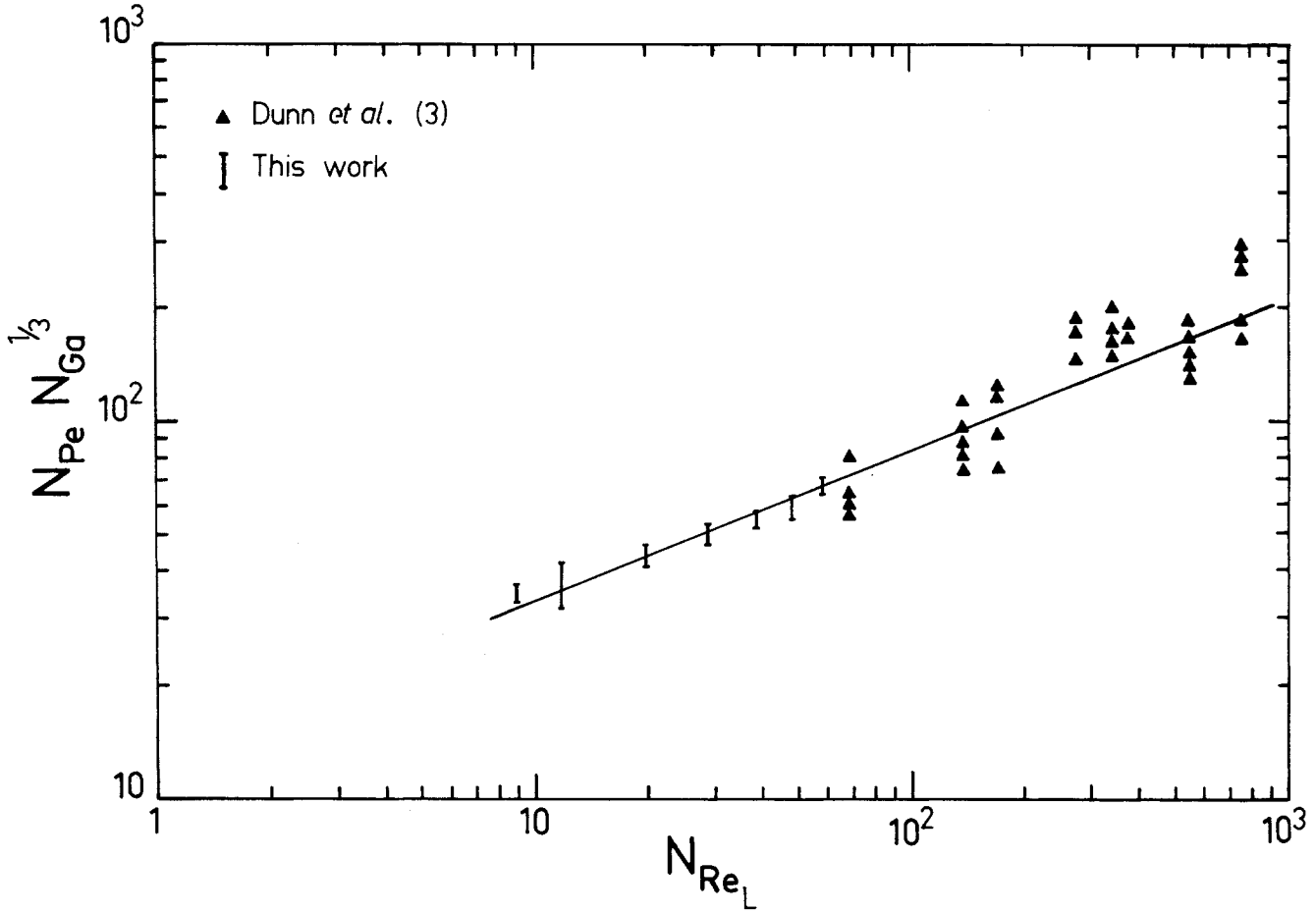

Fig. 6. $N_{Pe}\ N_{Ga}^{1/3}$ (N_{Pe} by least-squares fit) vs. Reynolds number.

forcing the result through the maximum point in the response curve.

Methods 1 and 2 lead directly to a Peclet number as shown in the Appendix. Computer programs written in FORTRAN II D were used to process the data collected on paper tape. These programs calculated the first and second moments, the mean residence time, and the variance; statistically checked the truncation; and were used for methods 1, 2, and 3.

The variance of the differences between the theoretical and measured response was compared with the variance of the noise in the system. An F and t test shows that there is a statistically significant difference between these variances, so the diffusion model can be rejected, since the differences between the theoretical and measured responses are larger than those due to the noise in the system. This applies for methods 1, 2, and 3. The principal difficulty in fitting the diffusion model to the response curve is the presence of the tail. This would indicate that a complex model would be suitable by combining the diffusion model with stagnant zones which contribute to the tail. Method 3 is an attempt to reduce the effect of the tail by forcing the theoretical result through the maximum of the response curve.

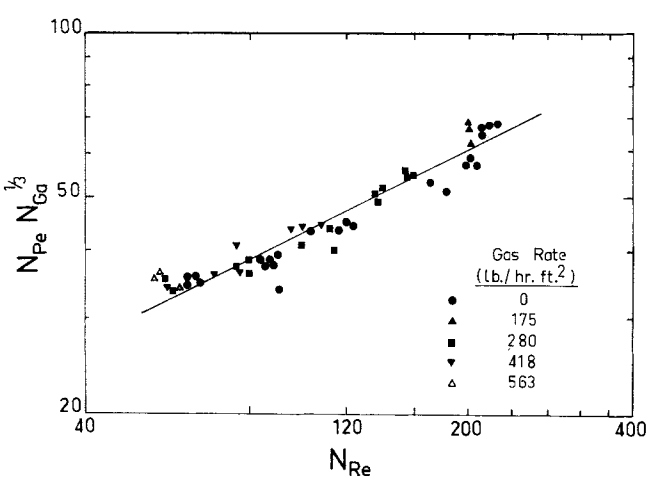

Fig. 7. $N_{Pe}\ N_{Ga}^{1/3}$ (N_{Pe} by least-squares fit) vs. Reynolds number based on interstitial velocity.

Figure 9 shows the Peclet number calculated by method 3 plotted against the liquid flow rate. There are over one hundred runs included on the figure covering all liquid and gas flow rates. To avoid confusion with such a large number of points, the mean values of the Peclet number and the limits $\pm 2\sigma$ have been given for the seven liquid flow rates. There are two important features of Figure 9 which should be noted. Firstly, there is a considerable reduction in scatter, and a curve can be drawn through the mean points. Secondly, there is a considerable increase in the Peclet numbers compared with those calculated from the second moments. Peclet numbers calculated by method 3 range from 0.25 to 0.5, whereas those by the second moment range from 0.02 to 0.15.

The results can be compared with the results of Dunn et al. by plotting $N_{Pe}\ N_{Ga}^{1/3}$ against the Reynolds number based on the liquid loading as shown in Figure 6. A correlation is given by

$$N_{Pe} = 13 N_{Re_L}^{0.4}\ N_{Ga}^{-1/3} \qquad (7)$$

When $N_{Pe}\ N_{Ga}^{1/3}$ is plotted against the Reynolds number

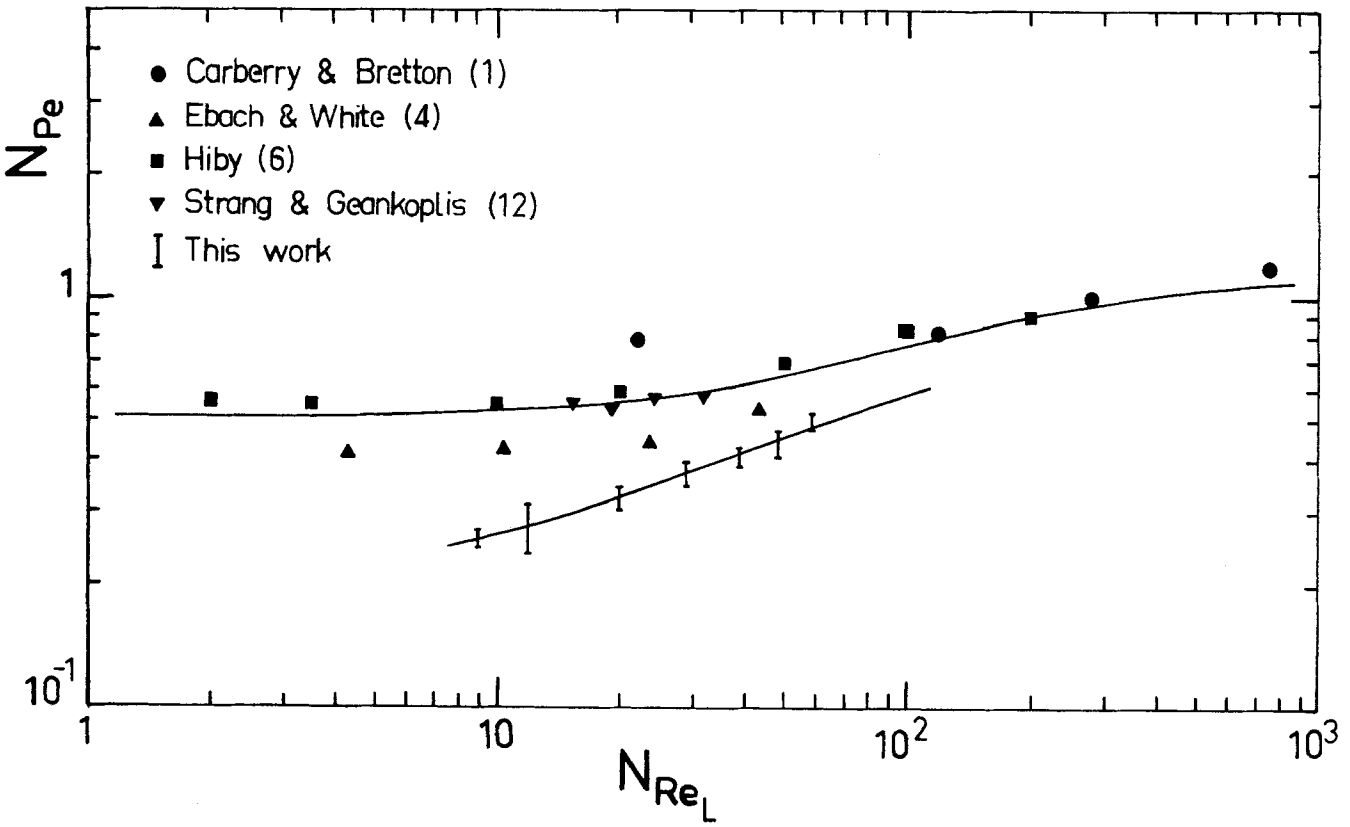

Fig. 8. Comparison of liquid-phase Peclet number by least-squares fit for two-phase flow with reported values of Peclet number for single-phase flow.

based on the interstitial velocity, as shown in Figure 7, a correlation is given by

$$N_{Pe} = 4.3\, N_{Re}^{1/2}\, N_{Ga}^{-1/3} \qquad (8)$$

This correlation is considerably higher than that given by Otake and Kunugita in Equation (6).

COMPARISON WITH SINGLE-PHASE RESULTS

Peclet numbers have been reported for single-phase liquid flow through ¼ in. Raschig rings or the nearest millimeter size by Otake and Kunugita (*9*), Carberry and Bretton (*1*), Ebach and White (*4*), Strang and Geankoplis (*12*), and Hiby (*6*). The results have been plotted in Figure 8, and Peclet numbers from 0.4 to 1.2 are covered over a range of Reynolds numbers based on the liquid loading from 2 to 1,000. The results reported here for two-phase flow are slightly below the single-phase results but may asymptote to them at high Reynolds numbers.

EFFECT OF THE GAS RATE

The gas rate was investigated from 0 to 99% of the flooding conditions over a wide range of liquid flow rates. The mean residence times increased by 5 to 10% for a gas flow rate of 280 lb./hr.sq.ft. A typical set of values for a liquid flow rate of 2,330 lb./hr.sq.ft. are 86.5 and 88.2 sec. which compare with 84.9, 84.4, and 81.6 sec. for a zero air rate.

The Peclet numbers calculated by method 3 are plotted on Figures 9, 6, and 7 for all gas flow rates. There does not appear to be any separation due to the gas rate even up to 99% of the flooding condition. A typical set of Peclet numbers for a liquid flow rate of 2,330 lb./hr.sq.ft. are 0.323, 0.320, and 0.332 for zero air flow and 0.294 and 0.322 for an air flow of 280 lb./hr.sq.ft., which is 55% of the flooding velocity. Results for a large numbers of runs at gas flow rates of 0, 175, 280, 418, and 563 lb./hr.sq.ft. are given on Figure 7. There is a tendency for the Peclet numbers to be slightly higher at higher gas flow rates, although the effect is not marked. The correlation of the results given by Equation (8), applies over a wide range of gas flow rates.

CONCLUSION

A feature of the literature results on liquid-phase dispersion is the considerable scatter when Peclet numbers are plotted against Reynolds number. Experimental measure-

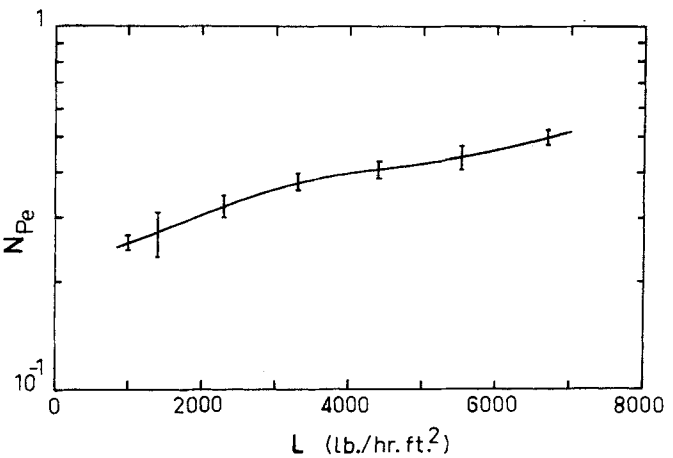

Fig. 9. Peclet number by least-squares fit vs. superficial liquid loading.

ments on ¼ in. Raschig rings in a 2 in. column also show this scatter when the Peclet numbers are evaluated from the second moment. If the Peclet number, calculated by minimizing the square of the differences between the theoretical and measured values and by forcing the result through the maximum point, is plotted against the Reynolds number, there is a considerable reduction in the scatter. Values of the Peclet number calculated by this method are larger than values calculated from the second moment. A correlation of the results is given by Equations (7) and (8).

The gas rate was investigated from 0 to 99% of the flooding condition over a wide range of liquid flow rates, and in this experimental column there was a negligible effect on the Peclet numbers.

ACKNOWLEDGMENT

R. W. Michell is supported by a Sydney University postgraduate research studentship.

NOTATION

a = surface area of the packing per unit volume of the column, sq.ft./cu.ft.
A_1 = constant $[\ln(Q/2\pi r^2\epsilon\sqrt{\pi D}) + Zu/2D]$
A_2 = constant $(-\frac{1}{2})$
A_3 = constant $(-Z^2/4D)$, hr.
A_4 = constant $(-u^2/4D)$, hr.$^{-1}$
C = concentration of tracer, lb./cu.ft.
d = nominal particle diameter, ft.
D = axial dispersion coefficient, sq.ft./hr.
g = acceleration due to gravity, ft./hr.^{2}
L = superficial liquid flow rate, lb./hr.sq.ft.
N_{Ga} = Galileo number, $d^3g\rho^2/\mu^2$
N_{Pe} = Peclet number, ud/D
N_{Re} = Reynolds number based on the interstitial liquid velocity, $du\rho/\mu$
N_{ReL} = Reynolds number based on the liquid loading, dL/μ
Q = amount of tracer added, lb.
r = radial distance coordinate, ft.
S = sum of squares, sq.lb./ft.^{6}
t = time, hr.
t_m = mean residence time, hr.
u = interstitial velocity, ft./hr.
x = axial distance coordinate, ft.
y = ln C, lb./cu.ft.
Z = length of bed, ft.
z_1 = ln t, hr.
z_2 = $1/t$, hr.$^{-1}$
z_3 = t, hr.
σ^2 = variance of response curve about mean
ϵ = void fraction
ρ = density of liquid, lb./cu.ft.
μ = viscosity of liquid, lb./ft.hr.

LITERATURE CITED

1. Carberry, J. J., and R. H. Bretton, *AIChE J.*, **4**, 367 (1958).
2. Danckwerts, P. V., *Chem. Eng. Sci.*, **2**, 1 (1953).
3. Dunn, W. E., et al., *Univ. Calif. Radiation Lab. Rept. 10394* (1962).
4. Ebach, E. A., and R. R. White, *AIChE J.*, **4**, 161 (1958).
5. Furzer, I. A., and G. Ho, *Chem. Eng. Sci.*, in press.
6. Hiby, J. W., *3rd Congr. European Fed. Chem. Eng. London*, C71 (June, 1965).
7. Hoogendoorn, C. J., and J. Lips, *Can. J. Chem. Eng.*, **43**, 125 (1965).
8. Kramers, H., and G. Alberda, *Chem. Eng. Sci.*, **2**, 173 (1953).
9. Otake, T., and E. Kunungita, *Kagaku Kogaku*, **22**, 144 (1958).
10. *Ibid.*, **4**, 251 (1966). (In English.)
11. Sater, V. E., and O. Levenspiel, *Ind. Eng. Chem. Fundamentals*, **5**, 86 (1966).
12. Strang, D. A., and C. S. Geankoplis, *Ind. Eng. Chem.*, **50**, 1305 (1958).
13. de Waal, K. J. A., and A. C. Van Mameren, *Chem. Eng. Progr. Symposium Ser. No. 6*, **60** (1965).
14. van der Laan, E. Th., *Chem. Eng. Sci.*, **7**, 187 (1958).
15. De Maria, Francesco, and R. R. White, *AIChE J.*, **6**, 473 (1960).

Manuscript received May 15, 1968; revision received October 25, 1968; paper accepted October 28, 1968.

APPENDIX

A mass balance for the tracer gives the following partial differential Equation (A1) which can be solved with suitable boundary conditions to give Equation (A2):

$$D\frac{\partial^2 C}{\partial x^2} - u\frac{\partial C}{\partial x} = \frac{\partial C}{\partial t} \tag{A1}$$

$$C = \frac{Q}{2\pi r^2\epsilon\sqrt{\pi D t}}\exp\left[-\frac{(Z-ut)^2}{4Dt}\right] \tag{A2}$$

Taking logarithms of Equation (A2), we get

$$\ln C = \ln\left(\frac{Q}{2\pi r^2\epsilon\sqrt{\pi D}}\right) + \frac{Zu}{2D} - \frac{1}{2}\ln t - \frac{Z^2}{4D}\cdot\frac{1}{t} - \frac{u^2}{4D}t \tag{A3}$$

This is of the form

$$y = A_1 + A_2 z_1 + A_3 z_2 + A_4 z_3 \tag{A4}$$

Consider the maximum point on the response curve (C_{max}, t_{max}) to be specified. Differentiating Equation (A2) with respect to t and equating to zero, we get

$$t_{max} = -\frac{D}{u^2} + \frac{D}{u^2}\left[1 - \left(\frac{Zu}{D}\right)^2\right]^{1/2} \tag{A5}$$

or

$$t_{max} = \frac{Z}{u} - \frac{D}{u^2} \tag{A6}$$

if

$$\frac{Zu}{D} >> 1$$

In terms of A_1, A_3, A_4

$$t_{max} = \sqrt{\frac{A_3}{A_4}} + \frac{1}{4A_4} \tag{A7}$$

or

$$A_3 = A_4 t^2_{max} + \frac{1}{16A_4} - \frac{t_{max}}{2} \tag{A8}$$

Writing Equation (A2) in terms of A_1, A_3, A_4 and substituting in Equation (A7), we get

$$A_1 = \frac{1}{2} - 2A_4 t_{max} + \ln\left(C_{max}\sqrt{t_{max}}\right) - \frac{1}{16A_4 t_{max}} \tag{A9}$$

Method 1 consists of finding by usual nonlinear regression techniques the curve of the form of Equation (A4) which best fits the experimental data.

Method 2 is essentially the same but with the additional condition that Equations (A8) and (A9) must hold.

In method 3, with the maximum point specified by Equations (A8) and (A9), A_4 is varied until

$$S = \sum_{i=1}^{n}\left[C_i - \exp\left(A_1 - \frac{1}{2}\ln t_i + \frac{A_3}{t_i} + A_4 t_i\right)\right]^2$$

is a minimum.